Monatshefte für Chemie 133, 829–836 (2002)

Monatshefte für Chemie
Chemical Monthly

Microstructure and Defect Characterization of Nanostructured Ni_3Al

Steven Van Petegem[1,*], **Danny Segers**[1], **Charles Dauwe**[1], **Florian dalla Torre**[2], and **Helena Van Swygenhoven**[2]

[1] Department of Subatomic and Radiation Physics, Ghent University, B-9000 Ghent, Belgium
[2] Nanocrystalline Materials Group, Paul Scherrer Institute, CH-5232 Villigen, Switzerland

Summary. Nanostructured Ni_3Al was produced by the inert gas condensation and *in situ* compaction technique and characterized by means of high-resolution transmission electron microscopy (HRTEM), X-ray diffraction, and density measurements. The defect structure was investigated using positron annihilation lifetime spectroscopy (PALS). It is shown that in some samples besides the cubic also the martensitic phase can be present. The defect structure can be divided into three major components: vacancy-like defects in the grain boundaries and nano-voids with a size of 1 nm as seen with PALS, and large pores with sizes up to 8 nm as seen with HRTEM. Furthermore, it is shown that an increasing compaction temperature leads to significantly smaller nano-voids.

Keywords. Nanostructures; Positron lifetime spectroscopy; Ni_3Al; Transmission electron microscopy.

Introduction

Ni_3Al is well known for its attractive high-temperature properties and consequent industrial applications (see *e.g.* Ref. [1]). It is also known that with a reduction of its grain size down to the nanometer scale, Ni_3Al exhibits enhanced mechanical properties like *e.g.* superplastic behaviour at low temperatures [2]. In the nanostructured regime defect structures constitute a non-negligible fraction of the solid and have therefore a big influence on its properties. In this work we present the characterization of the defect structures in nanostructured Ni_3Al produced by the inert gas condensation technique (IGC) using positron annihilation lifetime spectroscopy. Further structural characterization is done by high-resolution transmission electron microscopy (HRTEM), X-ray diffraction (XRD), and density measurements.

Positron annihilation lifetime spectroscopy (PALS) is a sensitive non-destructive tool to study defects in solids (see *e.g.* Ref. [3]). Positrons have the tendency to get trapped in open volume defects such as dislocations, vacancies, vacancy clusters, *etc.* This is due to the presence of an attractive potential at those

* Corresponding author. E-mail: steven.vanpetegem@rug.ac.be

defects. When trapped in such a defect, the lifetime of a positron increases as function of the defect size due to the lower electron density seen by the positron. Thus, probing the lifetime of a positron is equivalent to probing the size of the defects present in the solid. At large free volumes (>1 nm), positronium can be formed, which is a bound state of a positron and an electron, analogous to a hydrogen atom.

Results and Discussion

Sample characterization

Figures 1 and 2 show two typical X-ray diffraction spectra for Ni_3Al IGC samples. Sample A was compacted at room temperature, whereas sample B was compacted at 260°C. Figure 1 shows a diffraction pattern of a Ni_3Al sample with a rather 'pure' cubic structure. All three superlattice reflections {110}, {210}, and {211} show some increased intensity. The degree of ordering shows a value of 0.35, indicating 53% ordering compared to a fully ordered structure. No clear evidence can be found for the coexistence of another phase. Only one peak with a very small intensity not corresponding to the cubic phase fits to the {200} peak of the martensitic tetragonal phase of Ni_3Al. The intensity ratio between the {111} and the {200} peaks for both diffraction patterns of Figs. 1 and 2 shows a preferential orientation along the {111} planes.

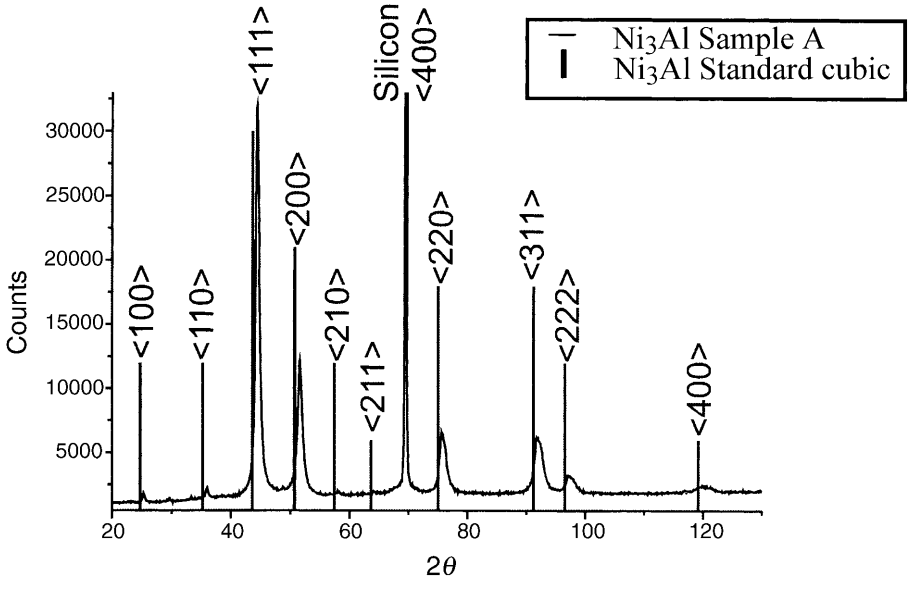

Fig. 1. X-Ray pattern of a Ni_3Al sample showing a rather 'pure' cubic microstructure; the peaks of the standard cubic Ni_3Al from the Joint Committee of Powder Diffraction Standards (JCPDS) database are added; a silicon wafer with an intense ⟨400⟩ peak at 69.4 2θ angle was added as a reference to correct for peak shifts

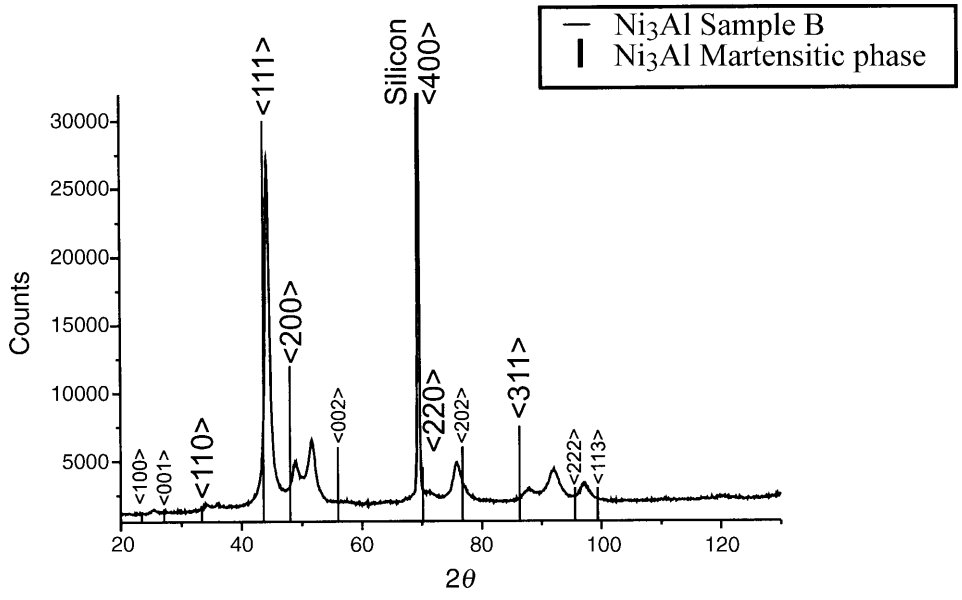

Fig. 2. X-Ray pattern of a Ni_3Al sample showing the cubic and the martensitic phase; the peaks of the standard martensitic Ni_3Al from the JCPDS database are added; the indices with small letters indicate that there is no detectable peak at this angle; a silicon wafer with an intense ⟨400⟩ peak at 69.4 2θ angle was added as a reference to correct for peak shifts

The diffraction pattern of Fig. 2 also shows ordering of the cubic structure (60% of full ordering). Additional to the peaks of the cubic phase, peaks of the martensitic phase, such as {110}, {200}, and {311} are clearly visible. The {111} peak of the martensic phase is not visible since it is superimposed on the {111} peak of the cubic phase. Further investigations showed that there is no correlation between the presence of the martensitic phase and the compaction temperature. Grain size measurements show roughly a mean grain size for sample A and B of respectively 18 and 11 nm and strains of respectively 0.558 and 0.509%. The lower grain size of sample B is probably due to the influence of the martensitic phase on the tail of the {111} peak.

In Figs. 3 and 4, HRTEM images of typical features that can be found in all samples are shown. They show a rather inhomogeneous microstructure with pores (Fig. 3) and big twins up to a size of 50 nm (Fig. 4). The untwinned grains have a mean size of about 15 nm, and grains as small as 4 nm could be observed. In Fig. 3 one can see the pores by the *Fresnel* contrast surrounding it. Pore sizes of 2 to 8 nm of elliptical shape could be found in this sample. The grains show a random orientation with mainly high-angle grain boundaries.

Corresponding to the HRTEM image of Fig. 3, a selected area electron diffraction pattern (SAED) with a selected area of approximately 500 nm can be seen in Fig. 5. The ring pattern shows the cubic phase of Ni_3Al with some ordering as seen by the reflections at {110}, {210}, and {210}. The {210} reflection is very week, indicating an incomplete ordering. No extra reflections of the martensitic phase could be found in this sample.

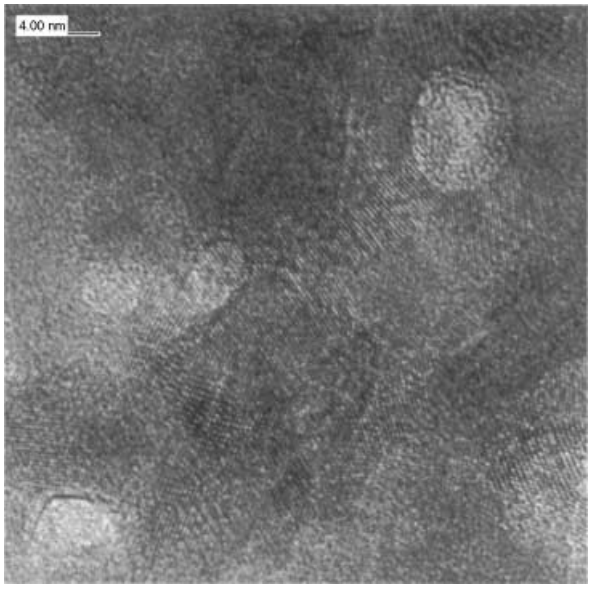

Fig. 3. HRTEM picture showing pores of about 4 to 7 nm surrounded by nanocrystalline grains

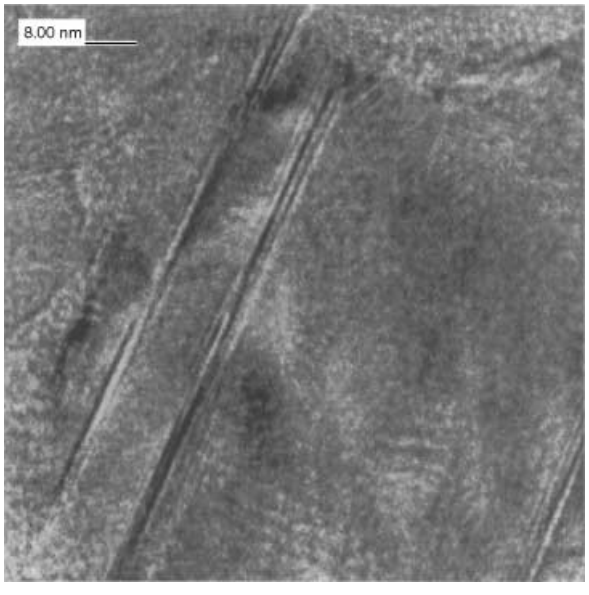

Fig. 4. HRTEM picture of twinned grains of about 50 nm

Positron lifetime spectroscopy

The positron lifetime in a well-annealed coarse-grained Ni_3Al sample was found to be 115 ± 1 ps. This value agrees well with data found in the literature (see *e.g.* Refs. [4, 5]). This is the lifetime of free delocalized positrons in perfect crystalline Ni_3Al. In an irradiated Ni_3Al sample a component of 181 ± 1 ps was

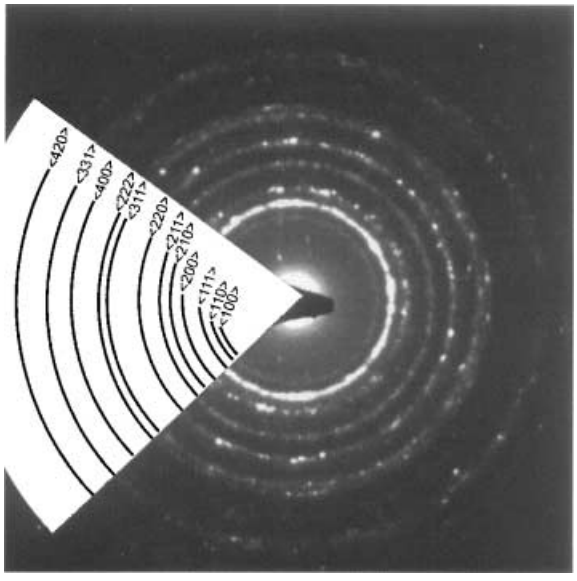

Fig. 5. SAED pattern of Ni_3Al showing some degree of ordering and no additional crystallographic phase

Table 1. Overview of positron lifetimes in nanocrystalline Ni_3Al compacted at room temperature at 2 GPa

	τ_1/ps	τ_2/ps	τ_3/ns	I_1/%	I_2/%	I_3/%
Sample 1	181±1	427±1	2.8±0.05	43±1	55±1	2.0±0.5
Sample 2	185±1	415±2	2.5±0.05	40±1	58±1	2.0±0.5

found. This is the lifetime of a vacancy in Ni_3Al. As the lifetime corresponding to a Ni and an Al vacancy only differs by a few ps [6], no distinction can be made between them.

The positron lifetime results of two nanocrystalline Ni_3Al samples are shown in Table 1. Both samples were prepared under the same conditions, *i.e.* pressed at room temperature at 2 GPa for 4 hours; their densities are 89% and 86% of that of bulk Ni_3Al. Three lifetimes could be distinguished, all of them being larger than the lifetime of free positrons in Ni_3Al. This is an indication that the defect concentration is high enough to trap all positrons into the defects. The consequence is that if more defects would be present, no change in relative intensities of the three lifetimes would be observed. This means that all information concerning the defect concentrations is lost. The shortest lifetime is comparable with the vacancy lifetime of the irradiated coarse-grained Ni_3Al sample. These defects are probably located at the grain boundaries, although one cannot exclude that some of them reside inside the grain as vacancies are stable at room temperature in Ni_3Al. In both samples a second lifetime of more than 400 ps was found. This is an indication for the existence of nano-voids. In order to estimate the size of these voids, lifetime calculations in well-known defects were performed in Ni_3Al [6]. From these

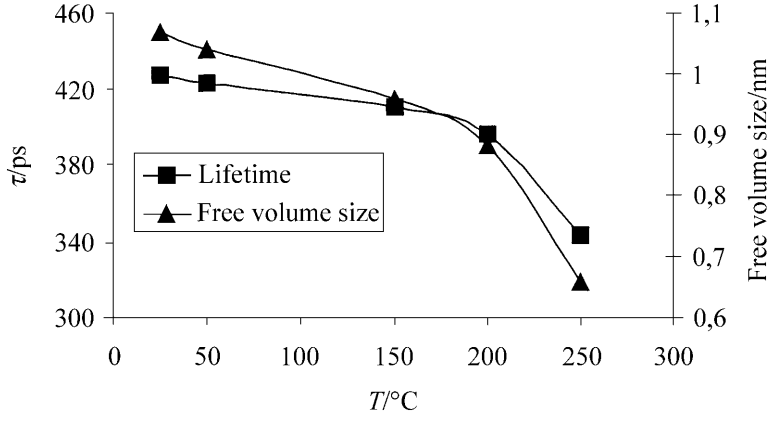

Fig. 6. Influence of the compaction temperatures on nano-void lifetime (τ_2)

calculations it was concluded that the nano-voids have a size of less than 1 nm. These small voids cannot be seen by HRTEM. The relative intensities indicate that more positrons annihilate in the nano-voids than in the vacancy-like defects. However, this is not an indication that the defect concentrations have the same ratio, as the trapping efficiency of nano-voids for positrons is much higher than of small defects. The third lifetime is due to the formation of *ortho*-positronium. No defect size estimations can be given for this component, as it is not possible to perform reliable positronium lifetime calculations in metals for the moment. This component probably originates from the pores in the sample.

In Fig. 6, the influence of the temperature during compaction on the second positron lifetime results is presented. The densities of the samples are all about 86% of that of bulk Ni_3Al. The size of the nano-voids decreases drastically to about 0.6 nm at 260°C. The lifetimes of the shortest component and of the positronium component did not change, neither did the intensities. At these temperatures, vacancies are not stable inside the grain; the shortest component therefore originates only from the grain boundary.

Conclusions

Nanocrystalline Ni_3Al produced by the inert gas condensation technique was characterised using XRD, HRTEM, and density measurements. It was shown that two phases can be present in the samples: the cubic phase, which was found in all samples, and the martensitic phase that could only be found in some samples. The HRTEM images revealed the existence of big twins (50 nm) and pores with a size up to 8 nm. Furthermore, it was shown that positron lifetime spectroscopy experiments on nanocrystalline materials can provide extra information about the defect structure that cannot be seen with other techniques. Here, three major defect structures were found: vacancy-like defects, nano-voids with a size of about 1 nm, and pores. Only the latter component could be seen using microscopy techniques. It was also shown that the compaction temperature has a major influence on the nano-voids.

Experimental

Sample preparation

A coarse grained Ni_3Al sample was produced by mixing high purity Ni and Al in a ratio of 3:1 at.% and subsequent annealing at 1600 K for 1 h. After mechanical and chemical polishing the sample was annealed at 1200 K for 100 h to obtain maximum homogeneity. The exact composition was determined as $Ni_{76}Al_{24}$. The sample was irradiated at room temperature with 2 MeV electrons at the LINAC facility [7] at the Ghent University with a dose of $1 \times 10^{18}\,e^-/cm^2$.

The nanostructured Ni_3Al samples were made by the inert gas condensation and *in situ* consolidation technique. A high-vacuum chamber (2×10^{-7} mbar) is filled with 3 mbar of high-purity (99.999%) helium. Pure cubic Ni_3Al is then evaporated from a resistively heated tungsten crucible. The evaporated atoms condense and form small clusters that are collected on a liquid nitrogen-cooled finger. The clusters are removed from the tilting cold finger with a copper scraper and then compacted under uni-axial pressure to produce disk-shaped samples of 8 mm diameter and 0.2–0.3 mm thickness. The compression unit is temperature controlled. The temperature is measured using a thermocouple close to the sample and is varied between room temperature and 260°C.

Characterization techniques

The density of the samples was measured *via* the *Archimedes* principle with a Mettler microgram balance. As reference, liquid diethyl phthalate with a density of $1.1175\,g/cm^3$ was used.

The X-ray measurements were made with a Siemens D500 X-ray detector. Applying the *Warren-Averbach* method after *Krill et al*. [8] for X-ray peak broadening, which is caused by small coherent domains, grain size and strain can be derived. Measurements were done on the $\langle 111\rangle/\langle 222\rangle$ family planes. A silicon wafer with an intense $\langle 400\rangle$ peak at 69.4 2θ angle was added as a reference to correct for peak shifts. In all samples a peak shift of about 0.5° towards higher 2θ angles was observed which is due to an instrumental artefact.

HRTEM investigations were carried out at the *Centre Interdepartemental de Microscopie Electronique* (CIME) at the EPFL, Lausanne, with a Phillips CM 300 instrument operating at 300 kV with a nominal resolution of 2 Å. The specimens were first mechanically pre-thinned and then electropolished in a double-jet Tenupol 3 apparatus using a solution of 10% perchloric acid in MeOH and operating at −30°C and 13.5 V yielding an approximate current of 0.135 mA. The degree of order of the cubic phase can be determined from the ratio between the intensities of the {110} superlattice reflection and the {220} fundamental line.

The positron annihilation lifetimes were measured using a conventional fast–fast lifetime spectrometer (see *e.g.* Ref. [3]) with a resolution (FWHM) of about 220 ps using the sandwich arrangement. The positron source (about 0.4 MBq) was obtained by evaporating $^{22}NaCl$ onto a standard kapton foil (7 μm thickness) which was then sealed with another foil. The number of counts in each spectrum (after background subtraction) exceeded 15×10^6. The spectra were analyzed using the multi-component program LT developed by *Kansy* [9]. All spectra could be decomposed into three components with a normalized χ^2 lower than 1.1.

Acknowledgements

The authors would like to thank Prof. *Pierre Stadelman* and Dr. *Marco Cantoni* from the CIME and Dr. *Robin Schaeublin* from CRPP, all at EPFL Lausanne, for their help in operating the HRTEM. We are also grateful to Dr. *Ivonna Jirásková* for supplying the coarse grained Ni_3Al samples. This research is part of the Interuniversity Poles of Attraction Program, Belgian State, Prime Minister's Office, Federal Office for Scientific, Technical, and Cultural Affairs (IUAP 4/10).

References

[1] Liu CT, Stringer J, Mundy JN, Horton LL, Angelini P (1997) Intermetall **5**: 579
[2] McFadden SX, Mishra RS, Valiev RZ, Zhilyaev AP, Mukherjee AK (1999) Nature **398**: 684
[3] Hautojärvi P, Corbel C (1995) Positron Spectroscopy of Defects in Metals and Semiconductors. In: Dupasquier A, Mills AP Jr (eds) Positron Spectroscopy of Solids. IOS Press, Amsterdam, p 491
[4] DasGupta A, Smedskjaer LC, Legnini DG, Siegel RW (1987) Mat Sci For **15–18**: 1213
[5] Mills AP, Wilson RJ (1982) Phys Rev A **26**: 490
[6] Van Petegem S, Kuriplach J, Hou M, Zurkin EE, Segers D, Morales AL, Ettaoussi S, Dauwe C, Mondelaers W (2001) Mat Sci For **363–365**: 210
[7] Mondelaers W, Van Laere K, Goedefroot A, Van den Bossche K (1996) Nucl Instr Met A **368**: 278
[8] Krill CE, Birringer R (1998) Phil Mag A **77**: 621
[9] Kansy J (1996) Nucl Instr Met A **374**: 235

Received October 5, 2001. Accepted (revised) November 12, 2001